



AFRL-RX-WP-TP-2009-4207

INFLUENCE OF RESIDUAL STRESSES ON FRETTING FATIGUE LIFE PREDICTION IN Ti-6Al-4V (POSTPRINT)

Patrick J. Golden, Dennis Buchanan, and Sam Naboulsi

Metals Branch

Metals, Ceramics, and NDE Division

JANUARY 2008

Approved for public release; distribution unlimited.

See additional restrictions described on inside pages

STINFO COPY

© 2008 ASTM International

**AIR FORCE RESEARCH LABORATORY
MATERIALS AND MANUFACTURING DIRECTORATE
WRIGHT-PATTERSON AIR FORCE BASE, OH 45433-7750
AIR FORCE MATERIEL COMMAND
UNITED STATES AIR FORCE**

REPORT DOCUMENTATION PAGE				<i>Form Approved</i> OMB No. 0704-0188	
The public reporting burden for this collection of information is estimated to average 1 hour per response, including the time for reviewing instructions, searching existing data sources, gathering and maintaining the data needed, and completing and reviewing the collection of information. Send comments regarding this burden estimate or any other aspect of this collection of information, including suggestions for reducing this burden, to Department of Defense, Washington Headquarters Services, Directorate for Information Operations and Reports (0704-0188), 1215 Jefferson Davis Highway, Suite 1204, Arlington, VA 22202-4302. Respondents should be aware that notwithstanding any other provision of law, no person shall be subject to any penalty for failing to comply with a collection of information if it does not display a currently valid OMB control number. PLEASE DO NOT RETURN YOUR FORM TO THE ABOVE ADDRESS.					
1. REPORT DATE (DD-MM-YY) January 2008		2. REPORT TYPE Journal Article Postprint		3. DATES COVERED (From - To)	
4. TITLE AND SUBTITLE INFLUENCE OF RESIDUAL STRESSES ON FRETTING FATIGUE LIFE PREDICTION IN Ti-6Al-4V (POSTPRINT)				5a. CONTRACT NUMBER In-house	
				5b. GRANT NUMBER	
				5c. PROGRAM ELEMENT NUMBER 62102F	
6. AUTHOR(S) Patrick J. Golden (AFRL/RXLMN) Dennis Buchanan (University of Dayton Research Institute) Sam Naboulsi (The University of Texas)				5d. PROJECT NUMBER 4347	
				5e. TASK NUMBER RG	
				5f. WORK UNIT NUMBER M02R3000	
7. PERFORMING ORGANIZATION NAME(S) AND ADDRESS(ES) Metals Branch (AFRL/RXLMN) Metals, Ceramics, and NDE Division Materials and Manufacturing Directorate Wright-Patterson Air Force Base, OH 45433-7750 Air Force Materiel Command, United States Air Force				8. PERFORMING ORGANIZATION REPORT NUMBER AFRL-RX-WP-TP-2009-4207	
9. SPONSORING/MONITORING AGENCY NAME(S) AND ADDRESS(ES) Air Force Research Laboratory Materials and Manufacturing Directorate Wright-Patterson Air Force Base, OH 45433-7750 Air Force Materiel Command United States Air Force				10. SPONSORING/MONITORING AGENCY ACRONYM(S) AFRL/RXLMN	
				11. SPONSORING/MONITORING AGENCY REPORT NUMBER(S) AFRL-RX-WP-TP-2009-4207	
12. DISTRIBUTION/AVAILABILITY STATEMENT Approved for public release; distribution unlimited.					
13. SUPPLEMENTARY NOTES Journal article published in <i>Journal of ASTM International (JAI)</i> , Volume 5, Issue 8 (September 2008). PAO Case Number: WPAFB 08-0086; Clearance Date: 16 Jan 2008. © 2008 ASTM International. The U.S. Government is joint author of this work and has the right to use, modify, reproduce, release, perform, display, or disclose the work. Paper contains color.					
14. ABSTRACT The objective of this work was to evaluate life prediction methodologies involving fretting fatigue of turbine engine materials with advanced surface treatments. Fretting fatigue tests were performed on Ti-6Al-4V dovetail specimens with and without advanced surface treatments. These tests were representative of the conditions found in a turbine engine blade to disk attachment. Laser shock processing and low plasticity burnishing have been shown to produce deep compressive residual stresses with relatively little cold work. Testing showed these advanced surface treatments improved fretting fatigue strength by approximately 50 %. In addition to advanced surface treatments, several specimens were also coated with diamond-like carbon applied through a nonline-of-sight process capable of coating small dovetail slots in an engine disk. Testing with this coating alone and combined with advanced surface treatments also significantly improved fretting fatigue strength due to a decreased coefficient of friction along with the compressive residual stresses.					
15. SUBJECT TERMS fretting, fatigue, crack growth, surface treatments, residual stress					
16. SECURITY CLASSIFICATION OF:			17. LIMITATION OF ABSTRACT: SAR	18. NUMBER OF PAGES 18	19a. NAME OF RESPONSIBLE PERSON (Monitor) James L. Larsen 19b. TELEPHONE NUMBER (Include Area Code) N/A
a. REPORT Unclassified	b. ABSTRACT Unclassified	c. THIS PAGE Unclassified			

Patrick J. Golden,¹ Dennis Buchanan,² and Sam Naboulsi³

Influence of Residual Stresses on Fretting Fatigue Life Prediction in Ti-6Al-4V

ABSTRACT: The objective of this work was to evaluate life prediction methodologies involving fretting fatigue of turbine engine materials with advanced surface treatments. Fretting fatigue tests were performed on Ti-6Al-4V dovetail specimens with and without advanced surface treatments. These tests were representative of the conditions found in a turbine engine blade to disk attachment. Laser shock processing and low plasticity burnishing have been shown to produce deep compressive residual stresses with relatively little cold work. Testing showed these advanced surface treatments improved fretting fatigue strength by approximately 50 %. In addition to advanced surface treatments, several specimens were also coated with diamond-like carbon applied through a nonline-of-sight process capable of coating small dovetail slots in an engine disk. Testing with this coating alone and combined with advanced surface treatments also significantly improved fretting fatigue strength due to a decreased coefficient of friction along with the compressive residual stresses. This work presents a mechanics based lifing analysis of these tests that takes into account the local plasticity and the redistribution of residual stresses due to the contact loading. The use of superposition of the residual stresses into the contact stress analysis results in unconservative crack growth life predictions. Finite element analyses were conducted to predict the redistribution of residual stresses due to the contact loading. The redistributed residual stresses were used to make improved crack growth life predictions when possible. The results showed very little redistribution of residual stresses for the advanced surface treatments, however, a significant change in shot peened residual stress gradients was predicted.

KEYWORDS: fretting, fatigue, crack growth, surface treatments, residual stress

Introduction

Fretting occurs in many aerospace components such as the dovetail attachments of turbine blades and disks in turbofan engines or lap joints in aircraft structures. Designers often seek palliatives such as coatings or shot-peening to reduce the negative effects of fretting on the life of a component. Typically, however, the positive effect of these palliatives is not taken into account in the design life of a component. Instead it may be treated as an additional margin of safety. As the retirement age of aerospace vehicles continues to grow, the expected maintenance cost and burden also continues to increase. This drives the need for new palliatives and design methods that will allow safe increases in component usage before repair or replacement. One option is advanced surface treatments such as laser shock processing (LSP) or low plasticity burnishing (LPB). These methods of inducing a layer of compressive residual stresses on a component, although more costly than shot-peening, may allow designers to use improved analysis methods to take credit for residual stresses in design as proposed by Prevey and Jayaraman [1], for example.

In order to take design credit for a process such as LSP or LPB it must be satisfactorily shown that the compressive residual stresses are sufficiently retained throughout the life of the component. Thermal relaxation, plastic deformation, or other sources of damage such as fretting or foreign object damage could all potentially reduce or even reverse the effects of the compressive residual stresses. It is known that plasticity in fretting contacts plays an important role in the understanding of crack nucleation and propagation of cracks. Waterhouse [2] observed that many antifretting palliatives may be disrupted by plastic deformations. Plastic deformation in the substrate of a coated material, for example, may result in a loss of coating adhesion and effectiveness. Intentionally induced compressive residual stresses by methods such as shot-peening could also be disrupted by this plasticity.

Manuscript received December 4, 2007; accepted for publication June 30, 2008; published online July 2008.

¹ Materials and Manufacturing Directorate, Air Force Research Laboratory, Wright-Patterson AFB, OH.

² Structural Integrity Division, University of Dayton Research Institute, Dayton, OH.

³ The Institute for Computational Engineering and Sciences, The University of Texas, Austin, TX.

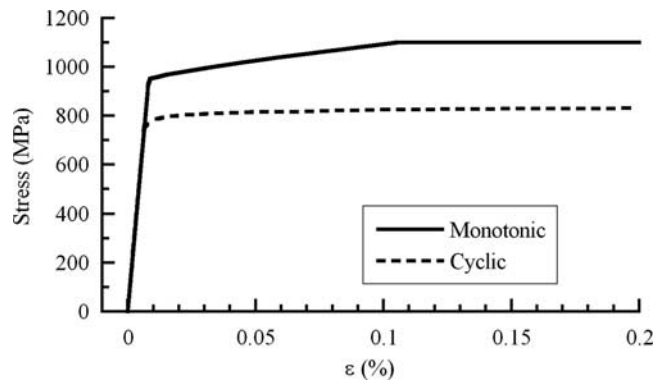


FIG. 1—Monotonic and cyclic stress versus strain curves used in the finite element analysis.

Martinez et al. have also proposed that the loss of residual stresses in a fretted material may be an indicator to fatigue damage [3]. Martinez et al. tested shot-peened fretting samples, some of which were interrupted prior to failure, and made an array of residual stress measurements on the surface across the fretting scar. The results showed that the compressive residual stresses relaxed in the fretted region. It appears that this may be a different mechanism than the local plastic zone being proposed in the current work since the relaxation appears over a wide region. Instead, accumulation of damage on the surface (microcracking, scarring, etc.) may be responsible for the relaxation of residual stresses throughout the fretted region. Since only surface residual stress measurements were taken, it is not clear if this was only a surface phenomenon or if relaxation extended into the depth.

In previous work, the current authors applied a mechanics based life prediction analysis to a series of fretting fatigue tests that included bare specimens, coated specimens, and specimens treated with LSP or LPB [4]. The conclusion of this work was that mechanics based predictions were accurate and conservative for bare Ti-6Al-4V specimens and also for coated specimens meaning that all of the predicted lives to failure were shorter than the actual lives to failure. In the LSP and LPB treated specimens, the fracture mechanics analysis predicted in all cases tested that short cracks would grow into a decreasing stress intensity factor range until crack arrest occurred. Thus, no specimen failures were predicted. In reality, several of the test specimens with LSP and LPB did fail, therefore, the predictions were not conservative. The objective of this paper was to investigate the possibility that redistribution of compressive residual stresses due to plastic deformations contributed to the nonconservative failure predictions in the LSP and LPB treated fretting specimens. A hypothetical shot-peened (SP) specimen was also analyzed. The influence of different levels of compressive residual stress retention was also studied. The approach was to conduct elastic-plastic contact finite element method (FEM) analyses to determine the level of plasticity and residual stress redistribution in the fretting experiments.

Experiments

The material used in this study was a Ti-6Al-4V alloy from the United States Air Force National High Cycle Fatigue program [5]. The material was $\alpha + \beta$ forged then solution treated and overaged at 932°C for 75 min, fan cooled, and mill annealed at 704°C for 2 h. The resulting microstructure was approximately 60 % primary α and 40 % transformed β . All of the test specimens were machined from this material. The elastic modulus was 116 GPa and the 0.2 % offset yield stress was 930 MPa. The ultimate tensile strength was 980 MPa. Monotonic and cyclic stress-strain curve fits were generated for this material and are plotted in Fig. 1. The cyclic stress-strain curve were fit to the stress-strain hysteresis loops from multiple strain controlled low cycle fatigue tests measured at the half life of the specimens. These stress-strain curves will be used in the elastic-plastic contact models described later.

A photograph of the dovetail fretting experimental setup is shown in Fig. 2. Development and testing with this fixture has been discussed previously by Conner and Nicholas [6] and Golden and Nicholas [7]. The steel fixture worked by pulling together a dovetail shaped test specimen and two fretting pads that had precisely machined surface profiles. Several surface profiles have been tested including cylindrical and flat with rounded edges with varying dimensions. All of the fretting pads in this work were machined to a flat with rounded edges profile with a 3 mm flat and 3 mm radii. There were several key features to this setup

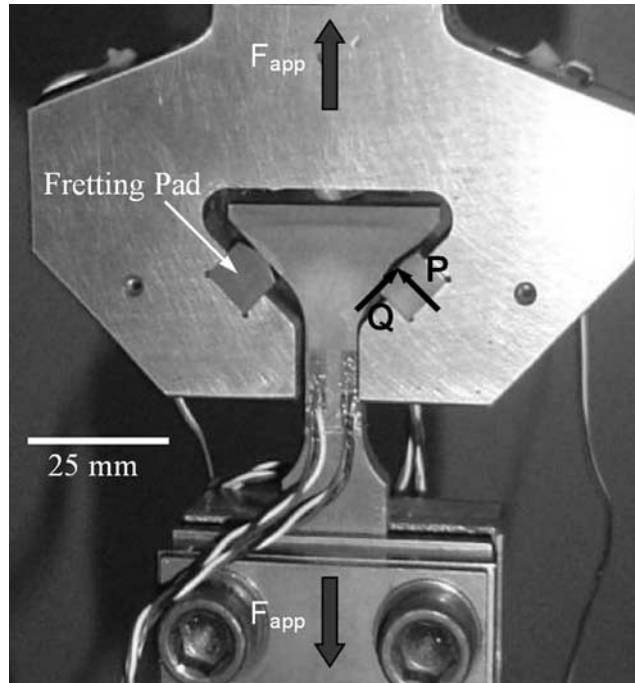


FIG. 2—*Photograph of the dovetail fretting fatigue setup.*

that separate it from other fretting fatigue apparatus. First, the specimen was dovetail shaped which resulted in cyclic loading of both the normal P and shear Q contact forces rather than only cyclic Q . Second, the fixture was designed with replaceable fretting pads. Each experiment only required replacement of the pads rather than the entire fixture as with other dovetail fatigue experiments [8]. Finally, it was not possible to obtain direct measurement of the contact forces P and Q unlike many other fretting fatigue test setups that do allow direct measurement of the contact forces through placement of load cells in the load path [9]. Instrumentation of the contact loads, however, was critical to allow validation of life prediction methods. Instrumentation was achieved through the addition of strain gages to the fixture in location of peak strain. Calibration of the contact forces to the strain gages was achieved through finite element modeling of the fixture as discussed in Golden and Nicholas [7].

The focus of this effort was to test and model the effects of coatings and residual stress surface treatments on dovetail fretting. LSP and LPB were each applied to six specimens in the regions of contact. Half of these and an additional five untreated specimen were also coated with diamond-like carbon (DLC). Several specimens were sent post-test for destructive measurement of the in-depth residual stresses. The measurements were made using x-ray diffraction in a region of the specimens just outside of the fretting scars. In-depth measurements were made by layer removal with electropolishing. The results were shown previously in Golden et al. [10] and curve fits of those results are plotted in Fig. 3. Also plotted is a typical residual stress profile of a shot-peened Ti-6Al-4V specimen peened with steel shot at 6–8 A intensity. These profiles were used in the stress analysis and life prediction described later. Note that the shot-peening profile has a significantly higher magnitude than both the LSP or LPB profiles, but the LSP and LPB processes provide a much deeper layer of compressive residual stress.

Room temperature tests at a load ratio $R=0.1$ were conducted at several load levels on bare Ti-6Al-4V, LSP treated, LPB treated, DLC coated, LSP+DLC, and LPB+DLC. The results were plotted in Fig. 4 and have been described previously in Golden et al. [10]. Both the residual stress treated specimens and the DLC treated specimens each extend the life by an order of magnitude. When DLC was combined with LSP or LPB none of the specimens were able to be failed. The fatigue load limit of the fixture was exceeded before failure of the specimens could occur. The contact loads and average friction coefficients for each of these tests were measured and will be used in the stress analysis and life prediction described below.

Analytical Procedures

Several different analysis procedures have been applied in this work. The overall objective of this research was to develop and demonstrate effective deterministic analysis methods that will allow accurate life

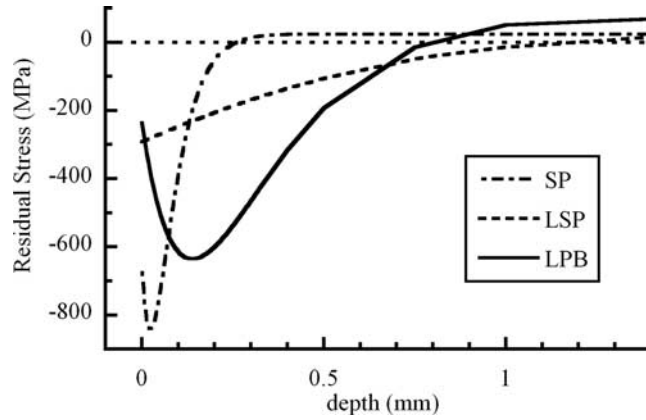


FIG. 3—Residual stress profile curve fits. The LSP and LPB curves were fit to measurements made in this work. The SP curve is fit to typical 6–8 A intensity peening data on Ti-6Al-4V.

prediction in a dovetail geometry. These methods accounted for changes in friction and residual stress due to surface treatments and processing. The mechanics based approach taken was dependent on the quality of the contact force measurement or prediction as well as the stress analysis tools. In this study, the contact forces were determined experimentally as discussed above. In general, however, the contact forces and the bulk stresses would be predicted from the results of a global FEM model. In either case, the local contact stresses were then calculated using the contact geometry and forces as input to a singular integral equation (SIE) solution (described below). In the case of applied surface treatments and/or local plasticity the residual stresses must be superimposed with the applied stresses. The effects of redistribution of residual stresses were a focus of the elastic-plastic contact modeling conducted in this work. Once the complete stress field had been calculated, standard nucleation and fracture mechanics life prediction methods were applied.

Figure 5 shows two schematics that represent the contact in the current experimental setup and the equivalent geometry used in the contact mechanics analysis. In the experiment, the dovetail specimen was pulled down into the contact pad, by force F . This results in the reaction forces P and Q and moment M (not shown) between the specimen and pad. The contact pad had a surface profile that was described by $h(x)$. In this case, the profile was a 3 mm flat with 3 mm radii at the edges of contact. In general, the configuration could have two materials; the specimen (E_1, ν_1) and the pad (E_2, ν_2), but in this study the

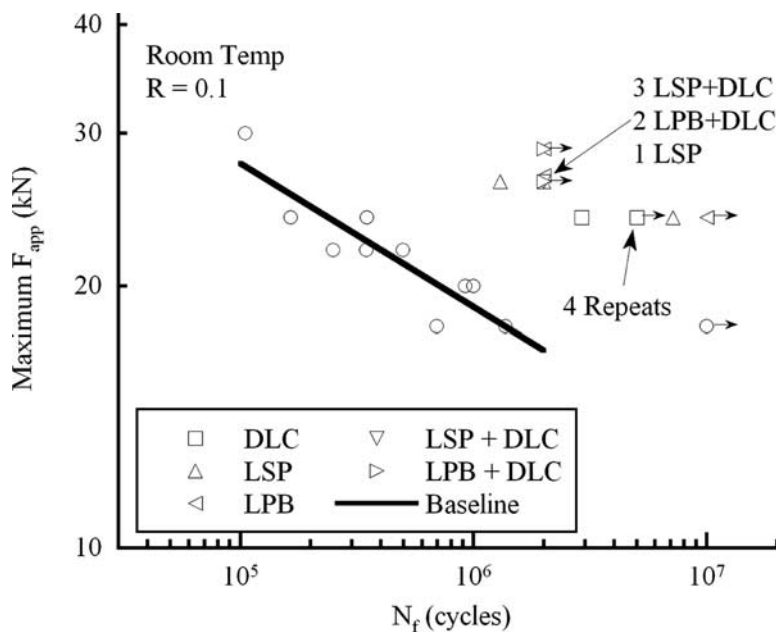


FIG. 4—Results of the dovetail fretting fatigue tests with advanced surface treatments and diamond like carbon coating.

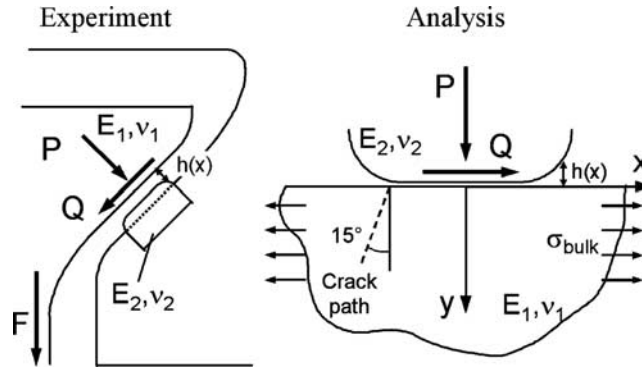


FIG. 5—Schematic of an equivalent geometric representation of an actual dovetail used in the singular integral equation solution to the contact problem.

materials were both Ti-6Al-4V. Although the contact forces were known from the experiment, the bulk stresses in the contact region were not. Prior studies [11,12] have described a method to extract the bulk stress from the FEM analysis in the contact region of a dovetail configuration. In short, the bulk stress was the FEM stress solution minus the contact stresses. Once the contact stresses were determined analytically as described below, they were subtracted from the FEM stress results to obtain the bulk stress. The reason a FEM and a SIE analytical solution were both used was that each had an advantage and a disadvantage in terms of accuracy and efficiency. The FEM solution accounted for all of the specimen or component geometric features and boundary conditions, whereas the SIE solution did not. The SIE solution was very fast and accurate at obtaining the very steep edge of contact stress gradient, whereas the FEM solution had long computational times and it was often not possible to obtain a converged stress solution at the edge of contact, particularly in three-dimensional models.

The second schematic in Fig. 5 shows the configuration used in the SIE analysis. A MATLAB script named CAPRI was used to solve the SIE that describes the contact between two similar materials with a gap function $h(x)$. CAPRI was written at Purdue University to calculate the normal and shear contact tractions and the subsurface stresses for an arbitrary indenter that is pressed into a semi-infinite body [13]. The influence of the bulk stress plays a role in the calculation of the contact tractions, but must be a known input and is not an output of the analysis. Thus, there is often a need for a FEM analysis to determine the bulk stress as described above. Once the SIE contact stress analysis including the bulk stress is complete, stress gradients can be extracted along the expected crack growth paths as shown in Fig. 5.

After the stress gradients were extracted the next step was to calculate nucleation and fracture mechanics stress intensity factor K . Nucleation was not the focus of this effort, however, an equivalent stress methodology to calculate nucleation life based on surface stresses had been applied in prior work [14]. This model includes the multiaxial components of stress and used a stressed area approach to account for the local stress peak at the edge of contact. K solutions were calculated using the weight function methodology. Mode I surface crack and through crack weight function K solutions were written in MATLAB to efficiently work with the output of CAPRI [11,15,16]. Negative K_I values were allowed to be calculated in the case of the residual stress gradients and were plotted in Fig. 6 and referred to as K_{RS} . Clearly negative values of K_{RS} are not real. They are only being used in combination with K_I calculated from the applied stresses to account for the change in stress state in the body and its affect on the crack due to the residual stresses. Superposition of K_{RS} with the maximum and minimum applied K_I resulted in a total ΔK_I that had a shift in R that was also a function of crack length. An effective stress intensity factor range, ΔK_{eff} , was then used to account for this changing R as calculated in Eq 1. Figure 7 is a plot of ΔK_{eff} versus crack size. Here, m is an exponent fit from crack growth data at R values of -1 , 0.1 , 0.5 , and 0.8 [5] and equals 0.72 for positive R and 0.275 for negative R . The crack growth rate and propagation life was then calculated from ΔK_{eff} using the sigmoidal crack growth law shown in Eq 2. Here B , P , Q , d , K_{th} , and K_c were constants fit to the crack growth data with values of -18.1 , 3.71 , 0.235 , -0.0066 , $4.21 \text{ MPa}\sqrt{\text{m}}$, and $66 \text{ MPa}\sqrt{\text{m}}$, respectively [5]. The crack growth rate da/dN data were in units of m/cycle

$$\Delta K_{eff} = K_{max}(1 - R)^m, \quad (1)$$

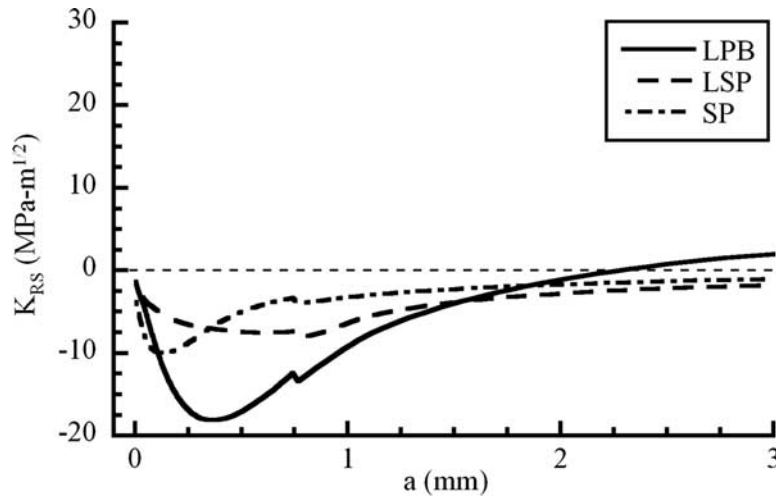


FIG. 6—Stress intensity factor due to residual stress gradients.

$$\frac{da}{dN} = 0.0254 \times \exp^B \left(\frac{\Delta K_{\text{eff}}}{K_{\text{th}}} \right)^P \left[\ln \left(\frac{\Delta K_{\text{eff}}}{K_{\text{th}}} \right) \right]^Q \left[\ln \left(\frac{K_c}{\Delta K_{\text{eff}}} \right) \right]^d. \quad (2)$$

A finite element model was generated to represent the dovetail fretting fatigue experiment loading conditions and is shown in Fig. 8. A simplified geometry of a two-dimensional (2D) plate and contact pad was chosen rather than modeling the actual dovetail geometry. The maximum and minimum contact forces, P , Q , and M , from the experiments were applied to the top surface of the contact pad in a cyclic manner. Five load cycles were found to be sufficient to stabilize the elastic-plastic response. Constraints were applied to the fretting pad to distribute the applied loads and to control its rotation. The bulk stress

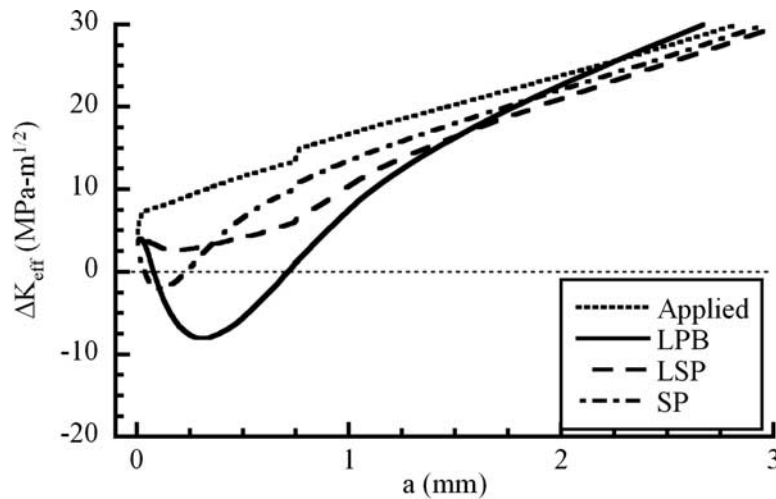


FIG. 7—Stress intensity factor range for combined applied load and residual stress.

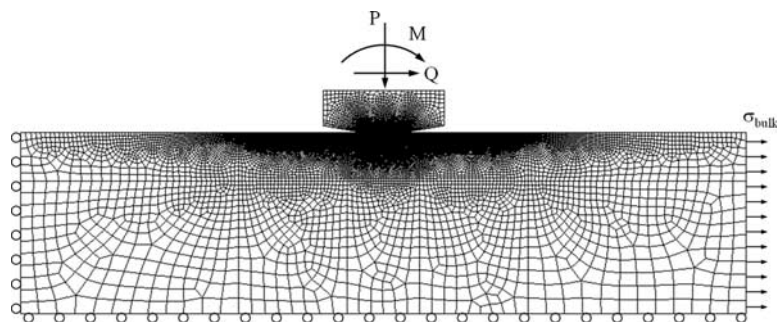


FIG. 8—Finite element model used to represent the loading conditions in the dovetail fretting tests.

was applied to the end of the plate, which represented the fretting specimen. The plate was 15 mm deep by 60 mm long and had roller constraints on the edges opposite the contact and bulk stress as shown in Fig. 8. The model was analyzed in ABAQUS and was meshed with 2D plane strain four-node bilinear elements. The element size in the contact region was 5 μm by 5 μm which was sufficient to capture the very high stress peaks at the edge of contact and the plastic zone that developed. The nonlinear combined isotropic/kinematic model provided in ABAQUS was used. The cyclic and monotonic stress strain curves plotted in Fig. 1 were the only data available for this analysis. The model was run using both sets of data with very little difference in results for these problems. The results shown in the following section were analyzed using the cyclic stress-strain curve.

Results and Discussion

The results of this work consist of the output of the elastic-plastic contact finite element analysis, changes in the residual stress profiles, and the resulting influence on life predictions. The life predictions in this work are focused entirely on crack propagation including short crack growth, rather than nucleation plus propagation. Prior work [17] has shown that at the end of interrupted fretting fatigue tests in Ti-6Al-4V cracks were often found very early in the expected life of the specimens. Also, nucleation life predictions on these experiments [11] have previously been shown to be on the order of 10 % of the total life or less. This was expected since the stresses at the edge of contact were typically well above yield in an elastic analysis, and then rapidly decreased. This led to early crack nucleation followed by relatively slow early crack growth. Additionally, all of the analysis in this work was limited to mode I fracture mechanics. Again, previous analysis on these experiments [11] as well as on other fretting fatigue experiments [18] have shown that any mode II contribution to crack growth was expected to be quite small. Although the calculated value of K_{II} was significant, ΔK_{II} was not. This, however, did not imply that all cracks grew perpendicular to the surface. In fact, the experiments showed that the macroscopic cracks grew approximately 15–25° from normal in a direction away from the center of contact. This was accounted for in the fracture mechanics calculations.

In these experiments, many of the treated specimens ended as run-outs and did not fail. It was predicted from the stress analysis, nucleation model, and fracture mechanics that despite the compressive residual stresses and/or the low friction coatings that cracks would still form at the edge of contact and grow a short length before arresting. This, in fact was the case as demonstrated in Fig. 9. Fig. 9 is a scanning electron microscopy micrograph showing a crack that grew from the edge of contact in a specimen treated with LPB. The section was mounted, ground, and polished in the specimen thickness direction. The crack was nearly 100 μm deep in this cross section which was near the maximum depth found for this crack. The fracture mechanics analysis with the El Haddad short crack correction [19] for this specimen predicts crack arrest at a depth of approximately 60 μm when the full residual stress gradient is superimposed with the applied stress gradient. The actual crack length is longer than the predicted crack arrest which is generally consistent with the unconservative fracture mechanics life predictions for these experiments that was discussed earlier. The observation of a crack in this and other run-out specimens did, however, validate the analytical results that showed cracks can nucleate, grow, and arrest under fretting fatigue. This has been observed in run-out tests with and without residual stresses due to LSP or LPB.

The contact finite element analysis with plasticity and initial residual stress distribution was conducted for the LSP, LPB, and SP conditions. Several different loading conditions were analyzed. These load cases used minimum and maximum values of P , Q , M , and bulk stress taken directly from the experiments. They were representative of the range from the least to most severe load cases found in the actual experiments. Multiple steps of maximum and minimum load were run until the plastic zone stabilized. Five cycles was found to be sufficient. Analyses with both the cyclic and the monotonic stress-strain curves were run and compared, but since the plasticity was so localized the difference was very small. The final result of interest was the change in the initial residual stress in the model, so the final load step in the analysis was unloading to zero applied loads. Fig. 10 is an example of redistributed shot-peen residual stresses in the specimen. The fretting pad is not shown. The surface to the right of the crack location is under the contact. The component of stress shown is the normal stress parallel to the surface. The effected zone was an approximately 300 \times 300 μm area at the edge of contact. It is observed that a significant amount of

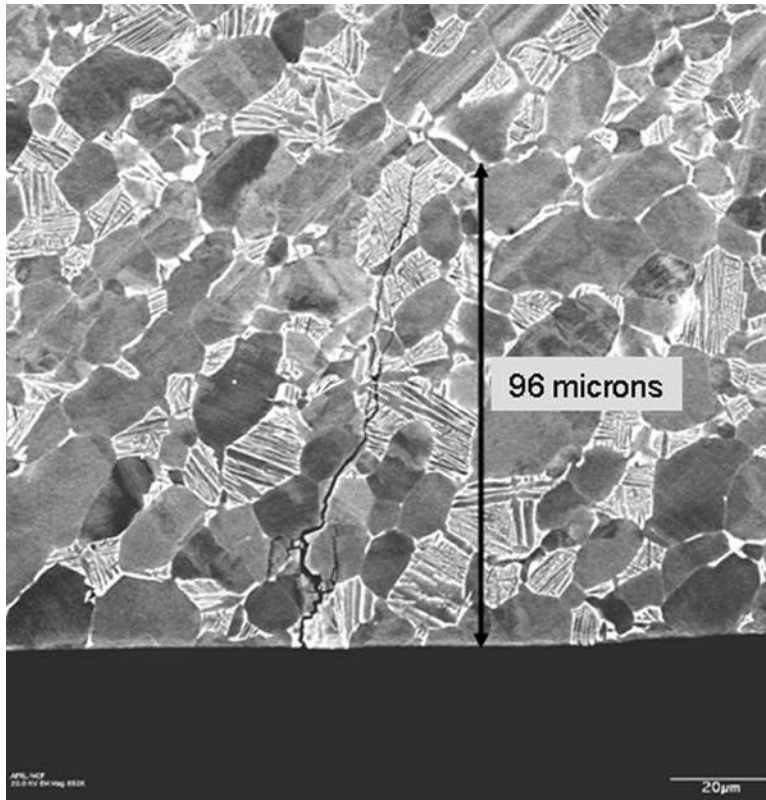


FIG. 9—Profile of a crack located at the edge of contact found post-test in a run-out experiment that had been processed with LPB.

redistribution was predicted to occur in this very small volume. This could significantly affect crack growth predictions for shot peened specimens in the short crack regime. A plot of the redistributed SP residual stress is shown in Fig. 11(a). This stress was taken along a path from the edge of contact into the

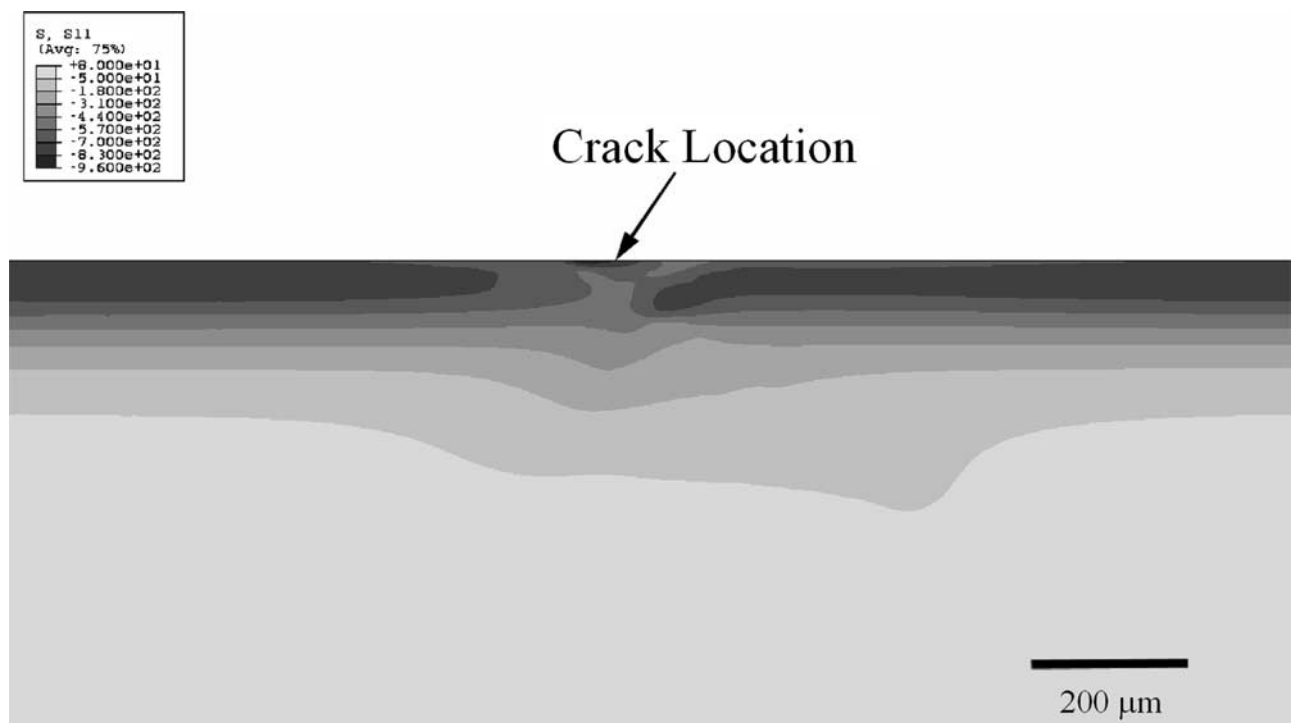


FIG. 10—Contours of shot-peen residual stress, σ_{xx} , at the edge of contact after stress redistribution. Contours range from +80 (light) to -960 MPa (dark) in 130 MPa increments.

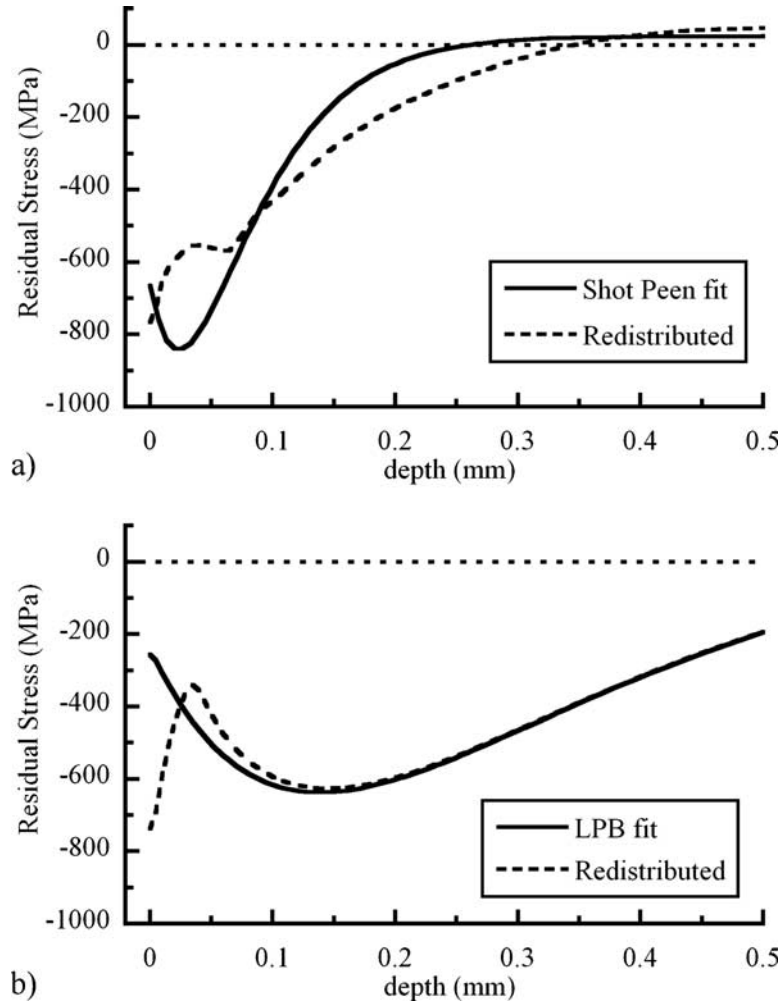


FIG. 11—Predicted redistribution of residual stress at the edge of contact for typical contact loading case for both (a) shot peening and (b) LPB.

depth and was compared to the original SP residual stress gradient. The distribution peak was significantly pushed into the tensile direction for the first 70 μm . This result is important because this peak is what is responsible for leading to potential early crack arrest and providing a fatigue benefit. Fig. 11(b), however, shows that for the LPB treated specimens a very different redistribution of the residual stress gradient occurred. The LSP treated specimens had a nearly identical trend. Here, the near surface stresses were pushed more compressive. Slightly deeper, the residual stress becomes more tensile to compensate.

The mechanisms for the different results in SP and LSP or LPB specimens can be explained as followed. The modeling showed that the high compressive stress due to contact during the negative shear reversal can combine with the compressive residual stresses to result in a localized plastic zone as was hypothesized. This can be observed in the finite element results shown in Figs. 10 and 11(a). The compressive yield results in a region of residual stresses that are shifted in the tensile direction near the surface (20 μm deep). Tensile yield occurs in the shot peened example [Fig. 11(a)] due to the high tensile stress due to contact during the positive shear reversal. This results in more compressive residual stresses at the surface (0–5 μm). The compressive yield zone was larger (60–70 μm deep) than the tensile, however, so there is a zone of more tensile residual stress (5–70 μm). Beyond 70 μm the residual stresses become more compressive to compensate. In the LPB treated samples, yielding was not predicted to occur during the negative shear reversal. The highest compressive stresses due to the applied loading occurred very near the surface, while the highest compressive residual stresses occur deeper in the material than those due to shot peening. The two compressive stress peaks (applied and residual) did not sufficiently overlap to result in a predicted plastic zone in the case of LPB. This is reflected in the predicted redistribution shown in Fig. 11(b). Here, the redistribution was caused entirely by the tensile yield that occurs at the surface in the edge of contact during the positive shear reversal. The compressive residual stresses due to LPB were smaller

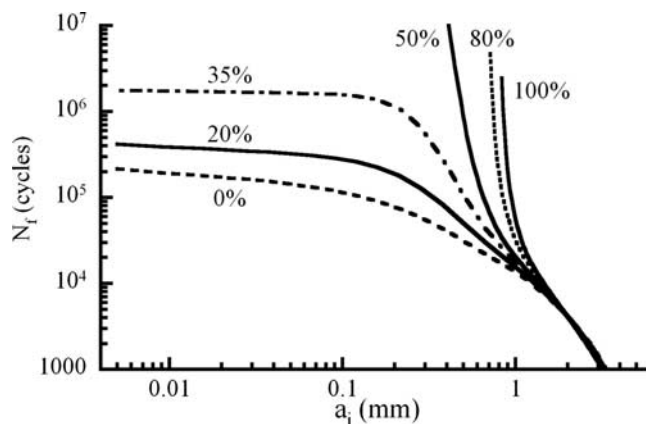


FIG. 12—Predicted remaining life as a function of crack length and percent retained residual stress due to LPB for a typical fretting experiment.

near the surface than those due to shot peening which also resulted in a larger predicted tensile plastic zone. Residual stress measurements of the specimens at the edge of contact were never performed. It was believed by the authors that the minimum x-ray spot sizes available using the x-ray diffraction technique were much too large to capture any expected localized change in residual stress. This may be an area of future work to either help confirm the analysis results or better explain the experimental results.

These predictions were based entirely on homogeneous material properties. The predicted plastic zone depths, however, were on the order of only a few grains. The local microstructure was not taken into account in the analysis. Goh et al. [20] showed that crystal plasticity may result in quite different results in predictions of localized plastic zones. In their simulations of plasticity under a fretting contact they showed that in the case of homogeneous material properties a small zone of cyclic plasticity develops surrounded by a larger zone that reaches an elastic shakedown condition. Much like the results predicted in this work. When the same material was modeled with crystal plasticity, however, a much deeper zone of ratcheting and cyclic plasticity was predicted. Although this type of analysis has not been conducted for the experiments in this work, Goh's results suggests that a more accurate analysis using crystal plasticity could result in a larger and deeper influence on residual stress redistribution.

The results of this work lead to the questions of how much of a reduction in the residual stress gradient is required to lead to life predictions that match the experimental results. Is a redistribution of residual stresses alone enough to explain the unconservative life predictions, or are some other sources of uncertainty in the analysis more important? To help answer these questions the life prediction analyses were repeated with different levels of residual stress gradients. The SP, LSP, and LPB gradients were each scaled to 100, 80, 50, 35, 20, and 0 % and the analyses were repeated for all of the respective fretting experiments. The SP gradients were applied to the uncoated LSP and LPB experiments for comparison since there were no shot peened experiments to analyze. An example of the results of this analysis is shown in Fig. 12. Crack growth to failure was predicted from a range of initial flaw sizes. In this example, 50 % of the LPB residual stress gradient or higher was predicted to result in no failure for initial crack depths smaller than approximately 0.5 mm. Shorter crack lengths were either below the crack propagation threshold or grew for a short time then arrested. Approximately 35 % of the LPB residual stress gradient resulted in a finite life prediction of approximately 2 million cycles. Since the actual specimen was a 10 million cycle run-out, the predicted remaining level of residual stresses in the specimen was between 35 and 50 %. A similar analysis was conducted on all of the LSP and LPB experiments and also the hypothetical SP samples. The predicted remaining level of residual stresses in the LSP specimens was 50–80 %. The predicted remaining level of residual stresses in the SP specimens that would result in some specimens failing was 35–50 %.

One additional observation from these analyses has been that the SP residual stress gradient could be predicted to be just as effective at preventing growth of fretting fatigue cracks as the LSP or LPB residual stress gradients. Even though the LPB gradient was much deeper than the SP gradient, it appeared that the magnitude and depth of the SP gradient is sufficient to prevent cracks of significant depth (0.3 mm) from growing in these experiments, if the original residual stresses remain unaltered. What the elastic-plastic

contact analysis in this work showed, however, was that the SP residual stress gradients appeared to be more easily altered due to redistribution from local plasticity than the LSP or LPB residual stresses. Additionally, prior research showed that shot peened Ti-6Al-4V was more susceptible to thermal relaxation than either LSP or LPB [21]. This was explained as being a result of the much higher level of cold work imparted on the material in shot peening than in LSP or LPB. A thorough understanding of the loading and thermal conditions and the possibility of tensile or compressive local yielding are important factors to consider when designing a fatigue critical location with SP, LSP, or LPB.

Conclusions

Mechanics based life predictions of LSP and LPB treated fretting fatigue experiments resulted in unconservative life predictions. An elastic-plastic contact analysis was conducted to determine the influence of plastic deformations on the residual stresses. The compressive stress from the applied loading at the edge of contact during the reverse shear cycle was predicted to be elastic under the test conditions in these experiments. When the applied compression was combined with shot-peening compressive residual stresses, however, a compressive yield zone formed that redistributed the compressive residual stresses in the tensile direction. This compressive yield zone did not form in the case of LSP or LPB treated samples because the peak compression was either deeper in the material or because the peak magnitude of compression was smaller than for shot-peening. Based on the results of the finite element modeling, it could not be concluded that redistribution of the residual stresses due to plasticity was the source of the unconservative life predictions on these experiments. Further analysis using crystal plasticity models, however, could reveal that local plasticity does result in redistribution of residual stresses in LSP or LPB.

The elastic-plastic contact analysis of shot-peened specimens showed a significant redistribution of the residual stresses at the edge of contact. Although no experiments were conducted with shot-peening in this work, this result suggests extreme caution must be applied before taking design credit for shot peening residual stresses with fretting.

Life predictions were conducted on all of the fretting experiments with different levels of retained residual stresses. Predictions were then made to determine the level of retained residual stresses that would make the predicted lives match the actual fretting fatigue lives. The level of retained residual stresses in the LPB specimens that correlated with the experimental results was 35–50 %. In the LSP specimens, the level of retained residual stresses that best correlated with the experiments was 50–80 %. This would be a significant reduction in residual stress that the analysis did not support. This lead the authors to believe that other sources of uncertainty besides the residual stresses not considered in the current deterministic analysis may be driving the unconservative life prediction results.

References

- [1] Prevey, P., and Jayaraman, J., “A Design Methodology to Take Credit for Residual Stresses in Fatigue Limited Designs,” *J. ASTM Int.*, Vol. 2, No. 8, 2005, Paper ID JA112546.
- [2] Waterhouse, R. B., “Plastic Deformation in Fretting Processes—A Review,” Hoepfner, D. W., Chandrasekaran, V., and Elliott, C. B., Eds., *Fretting Fatigue: Current Technology and Practices*, ASTM STP 1367, ASTM International, West Conshohocken, PA, 2000.
- [3] Martinez, S. A., Sathish, S., Blodgett, M. P., Mall, S., and Namjoshi, S., “Effects of Fretting Fatigue on the Residual Stress of Shot Peened Ti-6Al-4V Samples,” *Mater. Sci. Eng., A*, Vol. 399, 2005, pp. 58–63.
- [4] Golden, P. J., and Shepard, M. J., “Life Prediction of Fretting Fatigue with Advanced Surface Treatments,” *Mater. Sci. Eng., A*, Vol. 468–470, 2007, pp. 15–22.
- [5] Gallagher, J. P. et al., AFRL-ML-TR-2001-4159, “Improved High-Cycle Fatigue (HCF) Life Prediction,” Wright-Patterson Air Force Base, OH, January 2001.
- [6] Conner, B. P., and Nicholas, T., “Using a Dovetail Fixture to Study Fretting Fatigue and Fretting Palliatives,” *J. Eng. Mater. Technol.*, Vol. 128, 2006, pp. 133–141.
- [7] Golden, P. J., and Nicholas, T., “The Effect of Angle on Dovetail Fretting Experiments in Ti-6Al-4V,” *Fatigue Fract. Eng. Mater. Struct.*, Vol. 28, 2005, pp. 1169–1175.

- [8] Ruiz, C., Boddington, P. H. B., and Chen, K. C., "An Investigation of Fatigue and Fretting in a Dovetail Joint," *Exp. Mech.*, Vol. 24, 1984, pp. 208–217.
- [9] Hills, D. A., and Nowell, D., *Mechanics of Fretting Fatigue*, Kluwer, London, 1994, pp. 153–168.
- [10] Golden, P. J., Hutson, A. L., Sundaram, V., and Arps, J. H., "Effect of Surface Treatment on Fretting Fatigue of Ti-6Al-4V," *Int. J. Fatigue*, Vol. 29, 2007, pp. 1302–1310.
- [11] Golden, P. J., and Calcaterra, J. R., "A Fracture Mechanics Life Prediction Methodology Applied to Dovetail Fretting," *Tribol. Int.*, Vol. 39, 2006, pp. 1172–1180.
- [12] Rajasekaran, R., and Nowell, D., "Fretting Fatigue in Dovetail Blad Roots: Experiments and Analysis," *Tribol. Int.*, Vol. 39, 2006, pp. 1277–1285.
- [13] Murthy, H., Harish, G., and Farris, T. N., "Efficient Modeling of Fretting of Blade/Disk Contacts Including Load History Effects," *J. Tribol.*, Vol. 126, 2004, pp. 56–64.
- [14] Murthy, H., Rajeev, P. T., Farris, T. N., and Slavik, D. C., "Fretting Fatigue of Ti-6Al-4V Subjected to Blade / Disk Contact Loading," *Developments in Fracture Mechanics for the New Century*, 50th Anniversary of Japan Society of Materials Science, Osaka, Japan, 2001, pp. 41–48.
- [15] Shen, G., and Glinka, G., "Weight Functions for a Surface Semi-Elliptical Crack in a Finite Thickness Plate," *Theor. Appl. Fract. Mech.*, Vol. 15, 1991, pp. 247–255.
- [16] Glinka, G., and Shen, G., "Universal Features of Weight Function for Cracks in Mode I," *Eng. Fract. Mech.*, Vol. 40, 1991, pp. 1135–1146.
- [17] Hutson, A. L., Neslen, C., and Nicholas, T., "Characterization of Fretting Fatigue Crack Initiation Processes in Ti-6Al-4V," *Tribol. Int.*, Vol. 36, 2003, pp. 133–143.
- [18] Nicholas, T., Hutson, A., John, R., and Olson, S., "A Fracture Mechanics Methodology Assessment for Fretting Fatigue," *Int. J. Fatigue*, Vol. 25, 2003, pp. 1069–1077.
- [19] El Haddad, M. H., Smith, K. N., and Topper, T. H., "Fatigue Crack Propagation of Short Cracks," *J. Eng. Mater. Technol.*, Vol. 101, 1979, pp. 42–46.
- [20] Goh, C. H., McDowell, D. L., and Neu, R. W., "Plasticity in Polycrystalline Fretting Fatigue Contacts," *J. Mech. Phys. Solids*, Vol. 54, 2006, pp. 340–367.
- [21] Shepard, M. J., Prevey, P. S., and Jayaraman, N., "Effects of Surface Treatment on Fretting Fatigue Performance of Ti-6Al-4V," 8th National High Cycle Fatigue Conference, 2003.